Behavior of FRP-RC Slabs under Multiple Independent Air Blasts

Ganchai Tanapornraweekit, Ph.D.[1]; Nicholas Haritos[2]; and Priyan Mendis[3]

Abstract: In some terrorist attacks, it is possible that RC structures might be subjected to more than a single explosion. RC structures designed without the consideration of blast effects tend to lose their capacity after the first explosion. The use of a fiber reinforced polymer (FRP) sheet has been proven to enhance the performance and resistance of an RC member under a single explosion test. However, there appears to have been no experimental programs conducted to assess the performance of FRP-strengthened RC members subjected to multiple explosions reported in the literature. This paper, therefore, presents experimental results for the behavior of RC slabs strengthened by an FRP sheet after undergoing single, double, and triple independent explosion testing. Results from these blast tests indicate that the FRP sandwich RC slab tested was able to sustain the subsequent second explosion of greater impact. A brittle shear failure with FRP debonding was observed following the third explosion on this FRP-strengthened RC slab. **DOI: 10.1061/(ASCE)CF.1943-5509.0000191.**

CE Database subject headings: Fiber reinforced polymer; Blast loads; Explosions; Reinforced concrete; Concrete slabs.

Author keywords: Fibre reinforced polymer; Blast loads; Explosions; Reinforced concrete.

Introduction

The loss of life in terrorist bomb blasts is primarily a consequence of the actual physical effects of the collapse of structures and flying concrete debris. The research performed in this paper is, therefore, aimed at reducing the occurrence of concrete spalling and the failure of RC members that may lead to structural collapse under single and multiple explosions.

Fiber reinforced polymer (FRP) has been used extensively to strengthen RC members subjected to blast loads. Researches in the past have reported the performance of their FRP strengthened RC members tested under a single blast event (Crawford et al. 2001; Silva and Lu 2007; Wu et al. 2007; Ohkubo et al. 2008; Wu et al. 2009). However, no investigations of the efficiency of these composites members under the effects of multiple explosions appear to have been published. The term "multiple explosions" used in this paper refers to independent explosions in which blast waves from each explosion do not superimpose on one another forming a new blast wave, so must, therefore, be sufficiently separated in sequence in time.

[1]Researcher, Defence Technology Institute, 47/433, 4th Floor, Office of the Permanent Secretary of Defence Building, Chang Wattana Road, Pakkred, Nonthaburi 11120, Thailand; formerly, Ph.D. Student, Dept. of Civil and Environmental Engineering, Univ. of Melbourne, Melbourne, Victoria 3053, Australia (corresponding author). E-mail: ganchai.t@dti.or.th

[2]Associate Professor, Dept. of Civil and Environmental Engineering, Univ. of Melbourne, Melbourne, Victoria 3053, Australia. E-mail: nharitos@unimelb.edu.au

[3]Professor, Dept. of Civil and Environmental Engineering, Univ. of Melbourne, Melbourne, Victoria 3053, Australia. E-mail: pamendis@unimelb.edu.au

Note. This manuscript was submitted on April 29, 2010; approved on October 30, 2010; published online on December 3, 2010. Discussion period open until March 1, 2012; separate discussions must be submitted for individual papers. This paper is part of the ***Journal of Performance of Constructed Facilities***, Vol. 25, No. 5, October 1, 2011. ©ASCE, ISSN 0887-3828/2011/5-433–440/$25.00.

Experimental Study

A series of real blast tests was conducted in Thailand under a collaborative venture among the University of Melbourne, the Royal Thai Air Force (RTAF), and the Royal Thai Army (RTA) aimed at researching the feasibility of using FRP as a strengthening technique to enhance the performance of RC slabs under multiple explosions.

Details of Test Specimens and Strengthening Schemes

All the test slabs were cast with the same dimensions of 2,000 × 1,000 × 75 mm and the same layout of steel reinforcement. Fig. 1 presents the typical dimensions for these specimens and the details of their steel reinforcement.

For this paper, three types of FRP strengthening schemes, namely a single-sided FRP, a one layer FRP sandwich, and a two FRP layer sandwich, were investigated through a series of real blast tests conducted for this research. Both glass and carbon fiber sheets (GFRP and CFRP sheets) were employed to strengthen the test slabs in the test program. Table 1 lists all the strengthening patterns investigated in these blast tests.

Material Properties

In addition to the blast tests, static tests were employed to determine the mechanical properties of the concrete, steel rebars, and FRP sheets that were used in the blast test series. The material properties of concrete, steel, and FRP sheets obtained are presented in Tables 2 and 3.

Setup of Blast Tests

The test slabs in this series were supported in one direction by a steel test rig in which the trinitrotoluene (TNT) charge was suspended at a distance of 0.50 m above the test specimen, as shown in Fig. 2. The steel test rig was a modification of that previously presented by Wu et al. (2007). To prevent any significant settlement of the test rig, two RC band beams were constructed to stiffen and support the entire test rig assembly.

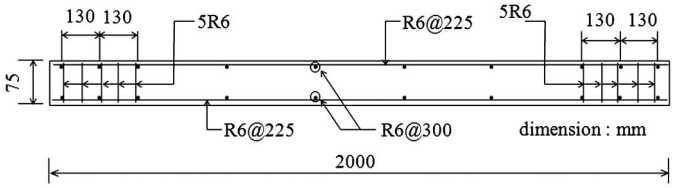

Fig. 1. Dimensions and reinforcement details of test slab

Table 1. Specimen Designations and Their Strengthening Schemes

Specimen designation	Description of strengthening schemes
C3, C4	without FRP strengthening
G-1S-1L	single-sided with one layer of GFRP sheet
G-2S-1L-a, G-2S-1L-b	one layer of GFRP sandwich
GC-2S-2L	one layer of GFRP sandwich and one layer of CFRP sandwich

Table 2. Material Properties of Steel and Concrete Under Static Tests

Properties	Steel	Concrete
Yield stress (MPa)	356	$f'_c = 32$ MPa
Ultimate strength (MPa)	412	
Strain at ultimate strength (%)	22.2	
Elastic modulus (GPa)	194	

Table 3. Material Properties of GFRP and CFRP Coupon Specimens Under Static Tests

Properties	GFRP	CFRP
Longitudinal Young's modulus, E_x (GPa)	75.6	235.2
Transverse Young's modulus, E_y (GPa)	17.7	21.6
Longitudinal tensile strength, X_t (MPa)	1,330	2,467
Transverse tensile strength, Y_t (MPa)	69	74
Longitudinal compressive strength, X_c (MPa)	547	890
Transverse compressive strength, Y_c (MPa)	262	366

Three lots of instrumentation were adopted in the tests to measure and estimate the displacement of the test specimens. These included a linear position sensor (LIPS), a set of mechanical devices adapted from eight television (TV) antennas, and a high-speed camera. The latter two items were used to extract the displacement data of the test specimen for the case in which the LIPS was removed from the test rig for its protection. Fig. 3 illustrates the setup of the LIPS and the TV antennas in the test program. The set of TV antennas could be used to estimate the maximum downward and upward deflections and also the peak deflected shape of the test specimen whereas the data from the high-speed video camera could be used to estimate the displacement-time history of the test slab for cases in which viewing conditions in the captured video frames were favorable. Because the pressure transducer was destroyed after the trial stage, no recorded pressure-time history results exist for all tests.

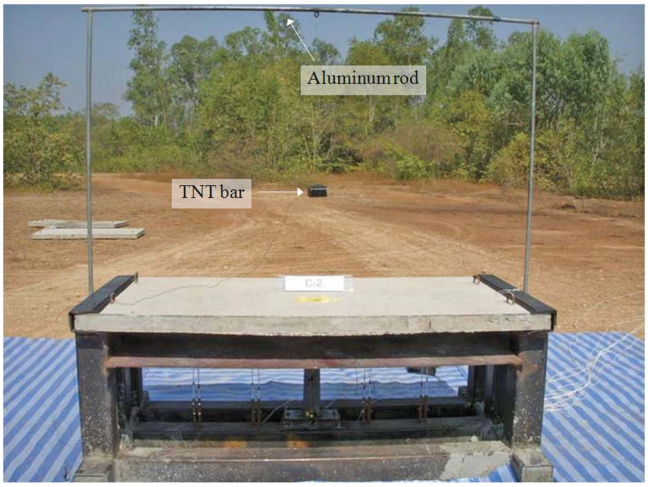

Fig. 2. Overall test setup (Image by G. Tanapornraweekit)

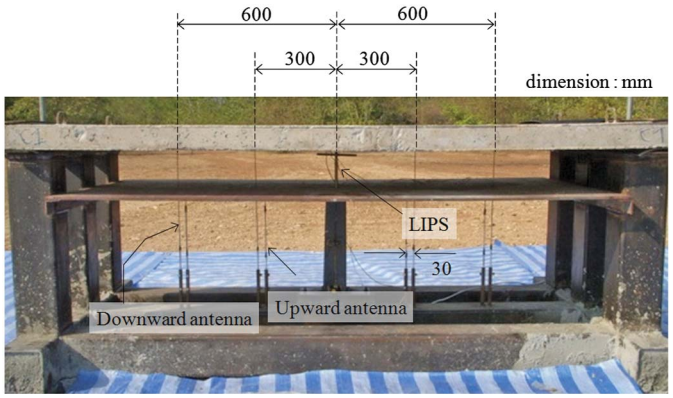

Fig. 3. Setup of LIPS and TV antennas (Image by G. Tanapornraweekit)

Table 4. Testing Sequence of Each Test Slab

Specimen	TNT charge weight, kg (scaled distance, m/kg$^{1/3}$)		
	First explosion	Second explosion	Third explosion
C3	0.45 (0.65)	—	—
C4	0.90 (0.52)	—	—
G-1S-1L	0.90 (0.52)	—	—
G-2S-1L-a and G-2S-1L-b	0.45 (0.65)	0.90 (0.52)	—
GC-2S-2L	0.45 (0.65)	0.90 (0.52)	1.35 (0.45)

Sequences of Testing

In the test program, control slabs without FRP strengthening, Specimens C3 and C4, and a single-sided FRP-RC slab, Specimen G-1S-1L, were subjected to a single blast test only. Multiple explosions were employed to test the single-layered and double-layered FRP sandwich RC slabs (Specimens G-2S-1L-a, G-2S-1L-b, and GC-2S-2L). Table 4 summarizes the testing sequences for all test specimens. The standoff distance for the charges used was kept constant at 0.50 m for all tests.

Experimental Results

Specimens C3 and C4

Specimen C3 was tested under the effects of a small explosion from 0.45 kg of TNT and obviously failed from a flexural failure. A single principal flexural crack was observed in the mid span of slab. In addition, there existed some smaller flexural cracks distributed along the span length of the test slab, as shown in Fig. 4. The maximum deflection of the slab was 47.4 mm, whereas its residual deflection was 30.2 mm, as measured by the LIPS. The recorded displacement-time history of Specimen C3 is compared with those of Specimens G-2S-1L-a and G-2S-1L-b in a subsequent section.

Specimen C4 was tested under the effects of a greater explosion from 0.90 kg of TNT. Because the effects of the explosion in this testing were rather severe, the LIPS was removed from the test rig because of safety concerns. Therefore, only the slab's residual deflection was physically recorded after the test.

The blast test showed that Specimen C4 failed in a combination of flexure and concrete spalling at the opposite face. Flexural failure was also observed because the slab deflected globally with large flexural cracks and almost collapsed, as shown in Fig. 5. In addition, concrete spall with dimensions of $200 \times 300 \times 25$ mm was observed at the opposite face of the test slab (see Fig. 6). The residual deflection of the test slab was measured to be 106 mm. The conclusion drawn from the testing of Specimens C3 and C4 was that the response of an identical test member shifts from a ductile to a brittle mode of failure by decreasing the blast scaled distance.

Fig. 4. Deflected shape and crack pattern of Specimen C3 (Image by G. Tanapornraweekit)

Fig. 5. Deflected shape and crack pattern of Specimen C4 (Image by G. Tanapornraweekit)

Fig. 6. Crack pattern and concrete spall on rear face of Specimen C4 (Image by G. Tanapornraweekit)

Specimen G-1S-1L

The one-sided GFRP-strengthened RC slab was subjected to a single explosion only from 0.90 kg of TNT. At this level of explosion, the LIPS was not installed because of safety concerns. Initially, the displacement of Specimen G-1S-1L during the slab vibration was intended to be measured from the video frames taken from the high-speed video. Unfortunately, the high-speed video did not function at the time of this blasting. However, a standard handy cam video, used as a backup, was able to capture some useful snapshots of the test slab motion. In the testing of this specimen, the only direct measurement approach employed to record the maximum deflection of the test slab was by way of a set of TV antennas.

After the explosion, Specimen G-1S-1L was observed to deflect upward toward the direction of the TNT charge. However, the specimen actually first slightly deflected downward in the direction of the applied blast pressures, as shown in Fig. 7. From a visual observation, this downward deflection was much smaller than that of Specimen C4 tested under the same level of explosion. This very small downward deflection was a consequence of the stiffening effect of the GFRP sheet applied on the opposite face of the test slab. Later in its response, the test slab rebounded with a higher displacement than its initial downward deflection. During the rebound stage, the incidence face of the test slab, therefore, experienced significant tensile stress. Because the GFRP sheet was not adhered to the incidence face, the concrete in that area was cracked easily. Therefore, the overall stiffness of the slab decreased, resulting in a large upward deflection. The deformed shape and crack pattern of this test slab is presented in Fig. 8. As shown in this figure, both the flexural and diagonal shear cracks were produced in the test slab.

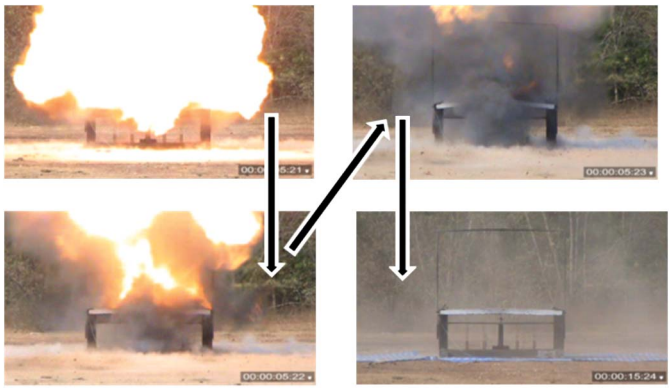

Fig. 7. Motion of Specimen G-1S-1L during blast test (Images by G. Tanapornraweekit)

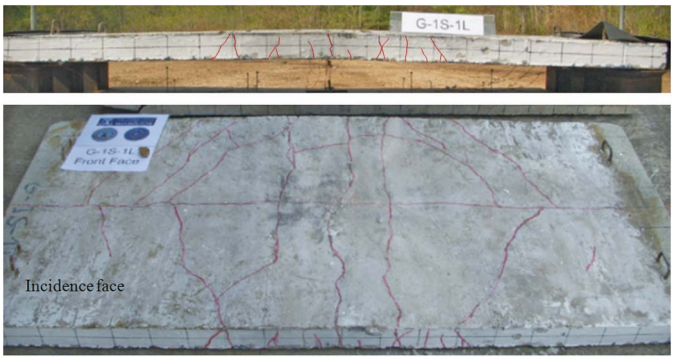

Fig. 8. Deformed shape and crack pattern of Specimen G-1S-1L (Image by G. Tanapornraweekit)

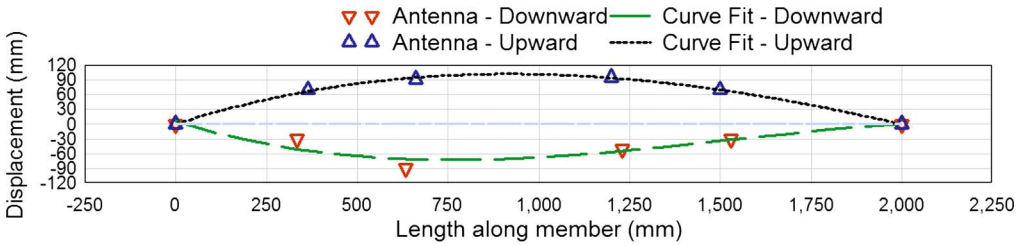

Fig. 9. Peak downward and upward deflections of Specimen G-1S-1L obtained from TV antennas

Because the LIPS was not installed on the test rig for this test, the maximum deflection of Specimen G-1S-1L was estimated from the video frames. The maximum upward deflection of Specimen G-1S-1L was approximately 75 mm; the residual upward deflection was 32 mm. However, the maximum upward deflection obtained from the captured photo frame might not have been the true value because the video camera may not have captured the frame when the maximum upward deflection actually took place. These estimated values were verified and compared with the values obtained from the TV antennas.

The peak downward and upward displacement could also be estimated from the peak values of the curves fitted to the data read from the TV antennas by using a second-order polynomial (see Fig. 9). These estimated peak deflections were compared with the data recorded from the LIPS in other specimens to verify the accuracy of this measurement technique. The approach with TV antennas was found to yield average errors of 23% and 14% for the peak downward and upward deflections, respectively. Assuming these errors, the peak downward and upward deflections reported from the TV antennas are in the ranges of 52–82 mm and 87–116 mm, respectively, for this specimen. The peak upward deflection of 75 mm from the video frames appears to be just under the 87–116 mm range implied by the TV antennas, suggesting that the actual maximum deflection was not captured by the available video frame in this instance.

Specimens G-2S-1L-a and G-2S-1L-b

These two specimens were nominally identical repeat test slabs that were strengthened by using the same GFRP sandwich scheme. The purpose of the repeated test was to verify the consistency and reliability of the test setup, the test measurements, and the standardization of the TNT used in the tests.

Testing Under First Explosion from 0.45 kg of TNT

The enhanced performance of the GFRP sandwich system was illustrated by a reduction in the maximum deflection of the test slab compared to the control slab without GFRP strengthening. Fig. 10 clearly indicates the capability of the GFRP sandwich to reduce the maximum and residual deflections of the test slabs in these blast tests. In addition, the frequency of the oscillations of the GFRP-RC slab increased compared to that of the control slab, providing another clear indication of the stiffening effect of this strengthening scheme. Although there appears to be some "shorting" anomalies in the record (i.e., occasional spikes) of Specimen G-2S-1L-a, the primary character of the displacement-time history is considered to have been captured reasonably well by the device.

Not only were the displacement-time histories of these two repeated GFRP-RC slabs very similar to one another but so also were their resultant crack patterns. The photographs presented in Fig. 11 show the similarity in the crack patterns of the two GFRP sandwich RC slabs. Small flexural cracks are shown to have propagated along the span length of the test slabs. The crack patterns that appeared on both faces of the GFRP sandwich slabs differed from those

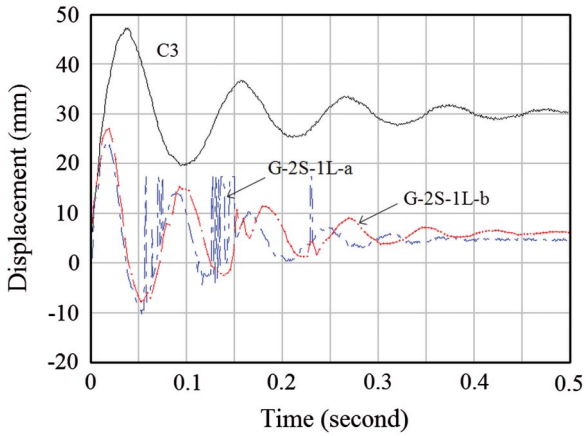

Fig. 10. Comparison of displacement-time histories of Specimens G-2S-1L-a, G-2S-1L-b, and C3 under first explosion

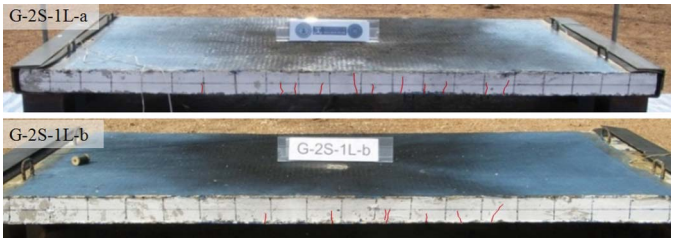

Fig. 11. Crack patterns and deformed shapes of Specimens G-2S-1L-a and G-2S-1L-b under first explosion (Images by G. Tanapornraweekit)

observed on the control specimen. Without GFRP strengthening, the control slab's principal damage was from the effects of the widening of the primary flexural cracks at the slab center, resulting in a large residual deformation. On the other hand, once the primary flexural cracks started propagating in the GFRP sandwich RC slabs, they were restrained by the GFRP sheets. Thus, to release the remaining energy from the blast impulses, the GFRP strengthened specimens had to find new easier paths for crack propagation. Therefore, the crack patterns in the GFRP sandwich specimens (see Fig. 11) appeared as multiple cracks in a smeared fashion instead of in the more discrete form of the control slab (i.e., Specimen C3).

Testing Under Second Explosion from 0.90 kg of TNT

Following the testing from their first explosion, Specimens G-2S-1L-a and G-2S-1L-b were subjected to a second round of explosions, resulting from a larger weight of TNT. During the second greater explosion, again, the LIPS was detached from the test rig because of safety concerns. Therefore, displacement-time history was not recorded for these tests. However, the video frames captured from the high-speed video camera were usable to estimate

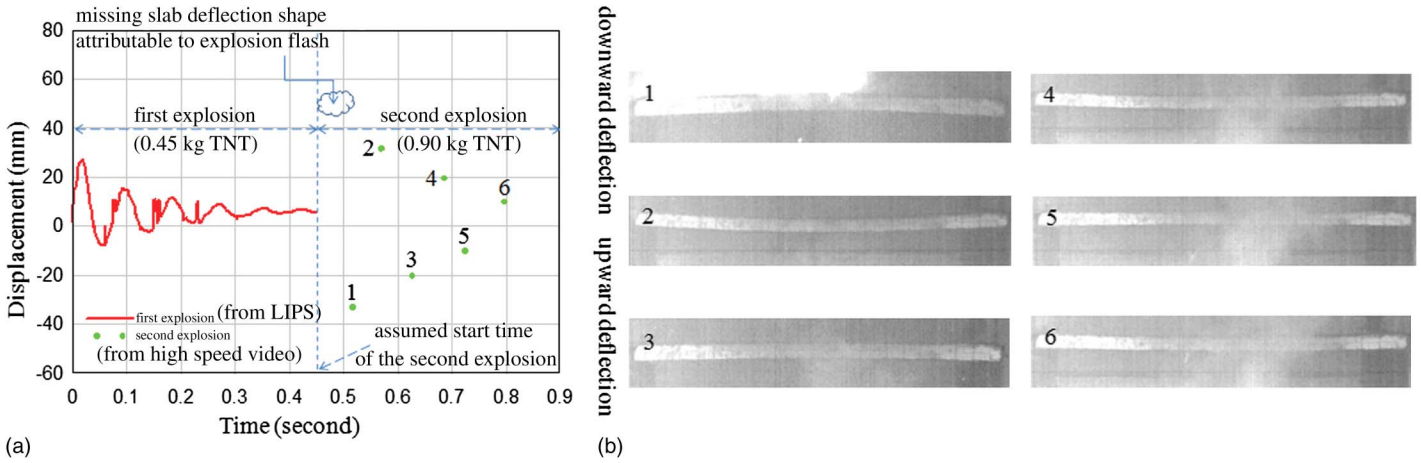

Fig. 12. (a) Deflection-time histories of Specimen G-2S-1L-b under first and second explosions; (b) video frames captured from high-speed camera during second explosion [Images courtesy of team of Science and Weapon System Development Center (SWSDC), Royal Thai Air Force (RTAF)]

the slab displacements in the time domain for these tests. Unfortunately, the first maximum downward deflection was missed because of the bright flash from the explosion.

The displacements of Specimen G-2S-1L-b under the second explosion estimated by using the high-speed video camera images were plotted onto the same graph of the displacement-time history for the same specimen under the first explosion, as presented in Fig. 12. The time of 0.45 s in Fig. 12 was the assumed detonation time of the second explosion, for presentation purposes, whereas the actual detonation time was approximately 15 min after the first explosion.

Fig. 13. Crack patterns and deformed shapes of Specimens G-2S-1L-a and G-2S-1L-b under second explosion (Images by G. Tanapornraweekit)

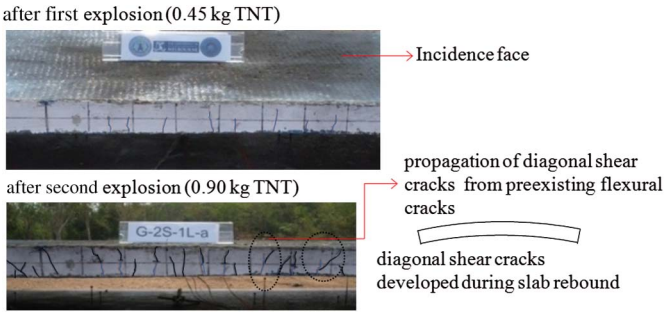

Fig. 14. Propagation of cracks in Specimen G-2S-1L-a under the 2nd explosion (Images by G. Tanapornraweekit)

The damage levels, deformed shapes, and crack patterns of these two specimens were similar to one another, as shown in Fig. 13. Under this round of explosion, the flexural cracks in both slabs propagated from the preexisting cracks caused by the first explosion to form full-depth flexural cracks through the slab thickness. In addition to the flexural cracks, diagonal shear cracks also propagated from the preexisting flexural cracks and also developed at some new locations, as shown in Fig. 14.

The direction of these diagonal shear cracks was opposite to those found in the unstrengthened RC slab under static load (MacGregor 1997), as shown in Fig. 15. Because the FRP sandwich RC slab largely behaved elastically, it deflected in both downward and upward directions in its dynamic response (refer to Fig. 12). Under the first downward movement of the slab, the concrete could still resist shear forces because the preexisting flexural cracks did not penetrate through the slab section. When the movement of the slab reversed, however, the flexural cracks propagated through the depth of the slab. During this stage, the deterioration of the concrete from the flexural cracks is believed to have compromised its ability to resist the developed dynamic shear forces. Therefore, diagonal shear cracks started to develop during the reversal phase. However, some minor diagonal shear cracks also followed the crack pattern typical of those resulting from a static loading of this type of slab (see Fig. 13). It appears that these conventional shear cracks developed during the first downward movement of the slab at the point at which the deterioration of the concrete was insignificant.

Specimen GC-2S-2L

Testing Under First Explosion from 0.45 kg of TNT

The two-layered GFRP-CFRP sandwich RC slab did not suffer any observable damage from the first explosion. Not even a single

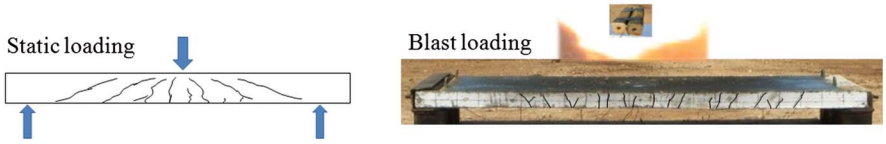

Fig. 15. Directions of diagonal shear cracks of RC members under static and blast loadings (Image by G. Tanapornraweekit)

Fig. 16. Specimen GC-2S-2L after first explosion (Image by G. Tanapornraweekit)

hairline crack was observed on the specimen after the test (see Fig. 16). Fig. 17 presents the displacement-time history of this two-layered GFRP-CFRP sandwich RC slab recorded by using the LIPS.

Testing Under Second Explosion from 0.90 kg of TNT

As was the case for the other 0.90 kg explosions, the LIPS was not attached to the test rig. Therefore, no direct displacement-time history was obtained for this specimen. Nonetheless, some data about the displacement of this specimen could again be estimated from the video frames captured by the high-speed video camera. Fig. 17 also presents the displacements of Specimen GC-2S-2L under the second explosion in which the detonation time of this round of explosion was assumed to be 0.45 s.

Fig. 18 shows the deformed shape and crack pattern of the test specimen after the explosion from 0.90 kg of TNT. Both flexural and diagonal shear cracks were observed on the side faces of the specimen after the test. The posttest observation indicated two patterns in the direction of the diagonal shear cracks of Specimen GC-2S-2L under the second explosion, as shown in Fig. 18. One diagonal shear crack followed the crack pattern typical of that resulting from static loading on such a slab whereas the direction of the adjacent diagonal shear crack was orthogonal to that of the previously mentioned shear crack.

Testing Under Third Explosion from 1.35 kg of TNT

The final test of Specimen GC-2S-2L was performed by using 1.35 kg of TNT. Under this highest-level explosion in this test program, none of the instruments were employed to monitor the displacement-time history of Specimen GC-2S-2L for safety reasons. Only the damage level and failure mode of the test slab were recorded.

After the detonation, the test slab failed from a combination of a large diagonal shear crack and the peeling of the FRP sheets on both the incidence and opposite faces to the blast. In addition, concrete spall was observed on the opposite face of the test slab. The fiber surface was burnt before the third explosion. Fig. 19 shows the failure of this specimen after the third explosion. From the posttest observations, the peeling of the top fiber sheet was deemed attributable to the large relative displacement resulting from the propagation of the primary diagonal shear crack near the support whereas the peeling of the bottom FRP sheet was deemed to have been initiated by the impact of fragmented concrete.

Fig. 18. Crack pattern and deformed shape of Specimen GC-2S-2L under second explosion (Image by G. Tanapornraweekit)

Fig. 19. Failure of Specimen GC-2S-2L after third explosion (Images by G. Tanapornraweekit)

Fig. 20. Shear failure of Specimen GC-2S-2L after third explosion resulting from shear crack initiated during the second explosion (Images by G. Tanapornraweekit)

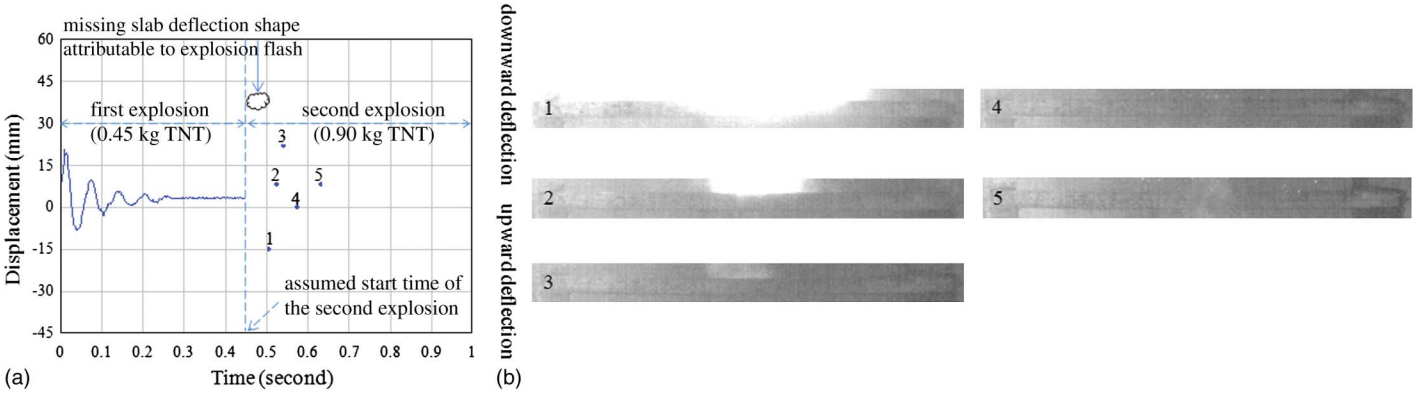

Fig. 17. (a) Deflection-time histories of Specimen GC-2S-2L under first and second explosions; (b) video frames captured from high-speed camera during second explosion [Images courtesy of team of Science and Weapon System Development Center (SWSDC), Royal Thai Air Force (RTAF)]

Table 5. Summary of Damage Levels and Crack Widths of Test Specimens Under First Explosion

Specimen	Damage level	Type of crack	Range of crack width (mm)
C3 (0.45 kg of TNT)	Moderate	Flexural cracks	0.05–0.5
C4 (0.90 kg of TNT)	Severe	Flexural/shear cracks and concrete spalling	0.5–20.0
G-1S-1L (0.90 kg of TNT)	Heavy	Flexural/shear cracks	0.05–1.8
G-2S-1L-a, G-2S-1L-b (0.45 kg of TNT)	Light	Flexural cracks	0.05
GC-2S-2L (0.45 kg of TNT)	No damage	No visible crack	—

Table 6. Summary of Damage Levels and Crack Widths of Test Specimens Under Second Explosion

Specimen	Damage level	Type of crack	Range of crack width (mm)
C3			
C4		No second explosion	
G-1S-1L			
G-2S-1L-a, G-2S-1L-b (0.90 kg of TNT)	Moderate	Flexural/shear cracks	0.1
GC-2S-2L (0.90 kg of TNT)	Light	Flexural/shear cracks	0.05

Shear failure in this blast event developed at the same location of the primary diagonal shear crack observed after the second explosion, as shown in Fig. 20. The diagonal shear crack that developed under the downward movement of the test slab caused the shear failure of the slab. Therefore, it can be implied that the test slab suddenly failed from shear failure without any slab vibration under the highest-level explosion. The specimen could perhaps have failed in a different failure mode had it been tested by using 1.35 kg of TNT immediately after the first explosion rather than after the second.

Although the two-layered FRP sandwich RC slab failed in a brittle manner from the third explosion, the specimen without FRP strengthening (i.e., Specimen C4) also failed from concrete spalling with a large deflection from a lower-level explosion. Therefore, the use of a suitable FRP strengthening system obviously enhances the performance of RC slabs subjected to blast loads.

Discussion of Efficiency of FRP Strengthening

The test results revealed that RC slabs with a single layer of GFRP sandwich are capable of resisting a second even larger explosion. Following the second independent explosion event, these strengthened RC slabs were still intact. In addition, the residual deflections of the FRP strengthened slabs after the first and second explosions were very small (refer to Figs. 11–13).

Experimental results showed that the maximum and residual deflections of the test RC slabs under explosions from 0.45 kg of TNT can be decreased by approximately 45% and 82%, respectively, as a result of strengthening with a single-layer GFRP sandwich scheme. The maximum and residual deflections can be further decreased by using a combination of a single-layer of GFRP and CFRP in the sandwich strengthening scheme. Reductions of 57% and 89% were reported for the maximum and residual deflections, respectively, for this latter configuration. Increasing the number of FRP layers does not linearly enhance the stiffness of the test member; only a marginal improvement was observed from the single FRP layer strengthening scheme when a second layer of FRP was used.

It appears that single-sided FRP strengthening also offers some advantages for RC slabs subjected to a blast load, although this strengthening is less effective than the FRP sandwich system. The single-sided strengthening scheme can still prevent the occurrence of the concrete spall that was observed during testing of the bare RC slab.

The test results obviously show that the crack widths in FRP-strengthened RC slabs were smaller than those of the slabs without FRP strengthening (refer to Tables 5 and 6). In addition, the damage levels in the FRP-RC slabs were less severe than those of the control slabs. Although no significant difference was observed in the displacement responses between the single-layered and double-layered FRP sandwich RC slabs, the latter strengthening scheme is more efficient in controlling the crack distribution and crack widths in RC slabs.

Conclusions

The efficiency of three FRP strengthening schemes for improving the blast performance of RC slabs under multiple explosions was examined for this paper. A single-sided FRP, a single layer FRP sandwich, and a double-layer FRP sandwich strengthening schemes were investigated through a series of real multiple explosion tests. The single-sided FRP strengthening scheme prevented the concrete spalling observed in the bare RC slab subjected to the same level of explosion. However, this type of strengthening was not as effective as that offered by the single-layer FRP sandwich strengthening scheme. The FRP sandwich RC slabs were still intact after the second explosion. In addition, the deformed shapes of the FRP-RC slabs were not different from those observed before the tests.

A triple explosion test was performed on the double-layered FRP sandwich RC slab. Under the first two explosions, the test slab performed very well; the damage of the test slab was very light. A small number of cracks was observed on the test slab. The preexisting diagonal shear crack initiated during the second explosion led to shear failure and subsequent FRP delamination following the third, highest level of explosion. In addition, concrete spalling was observed after this explosion. Although the test slab with two layers of FRP sandwich failed in a brittle manner after this third explosion, the bare RC slab was observed to fail from concrete spalling under a smaller level of explosion.

In conclusion, both the one- and two-layer FRP sandwich strengthening schemes were very effective in improving the ductility of the test slabs and enabling the test slab to survive the blast effects from a subsequent explosion.

References

Crawford, J. E., Malvar, J, Morrill, K. B., and Ferritto, J. M. (2001). "Composite retrofits to increase the blast resistance of reinforced concrete buildings." *Proc., 10th Int. Symp. on Interaction of the Effects of Munitions with Structures*, San Diego, 1–13.

MacGregor, J. G. (1997). "Reinforced concrete: Mechanics and design." *Shear in beams*, Prentice Hall, Upper Saddle River, NJ, 180–231.
Ohkubo, K., Beppu, M., Ohno, T., and Satoh, K. (2008). "Experimental study on the effectiveness of fiber sheet reinforcement on the explosive-resistant performance of concrete plates." *Int. J. Impact Eng.*, 35(12), 1702–1708.
Silva, P. F., and Lu, B. (2007). "Improving the blast resistance capacity of RC slabs with innovative composites materials." *Composites, Part B*, 38(5–6), 523–534.
Wu, C., et al. (2007). "Blast testing of RC slabs retrofitted with NSM CFRP plates." *Adv. Struct. Eng.*, 10(4), 397–414.
Wu, C., Oehlers, D. J., Rebentrost, M., Leach, J., and Whittaker, A. S. (2009). "Blast testing of ultra-high performance fibre and FRP-retrofitted concrete slabs." *Eng. Struct.*, 31(9), 2060–2069.